中国科学院高能物理研究所
Institute of High Energy Physics
Chinese Academy of Sciences

Muonium-to-Antimuonium Conversion Experiment

Positron Detection System of Muonium-to-Antimuonium Conversion Experiment

Presenter: Huaxing Peng

penghuaxing@ihep.ac.cn

2025.9.16

Content

- Background
- Experiment setup and method
- Performance testing of the positron detection system
- Conclusion

Background

- We focuses on the charged lepton flavor violation (cLFV) through the investigation of muonium-to-antimuonium conversion (M-to-$\overline{M}$).
- M-to-$\overline{M}$ conversion is identified by coincident fast e$^-$ and slow e$^+$ events.

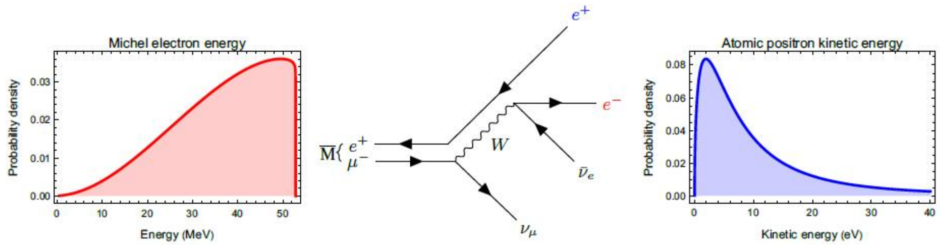

(a) e$^-$ energy spectrum (b) Leading-order $\overline{M}$ decay (c) e+ energy spectrum

Fig. 2 Energy spectrum and the diagram of antimuonium decay $\overline{M} \to e^+e^-\nu_e\nu_\mu$

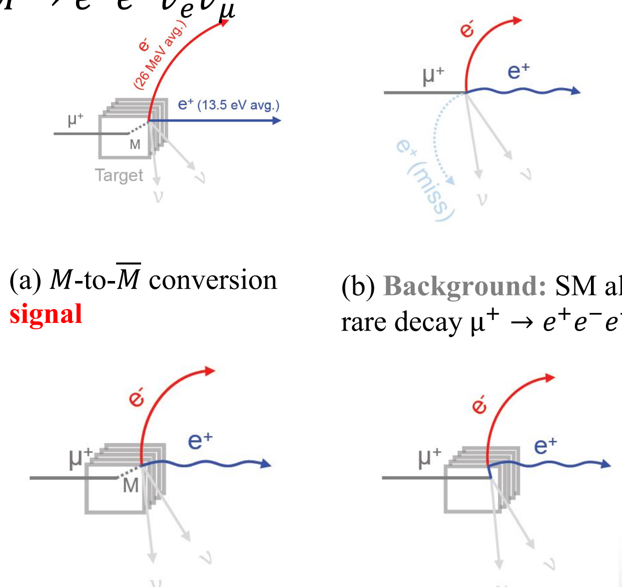

(a) M-to-$\overline{M}$ conversion **signal**

(b) **Background:** SM allow rare decay $\mu^+ \to e^+e^-e^+\nu_e\overline{\nu_\mu}$.

(c) **Background:** muonium decay with Bhabha scattering.

(d) Accidental **backgrounds**

Fig. 3 Event topologies for signals and backgrounds.

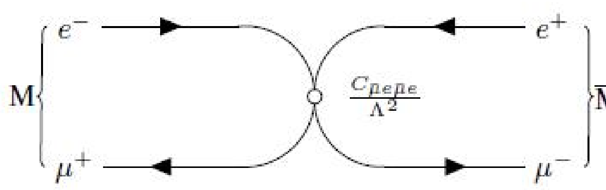

Fig. 1 The SMEFT tree-level diagram for muonium-to-antimuonium conversion with one $\Delta L_\mu = 2$ four-fermion effective vertex.

Background

Muonium-to-Antimuonium Conversion Experiment (MACE) is proposed

M-to-$\bar{M}$ P ≤ 8.3×10^{-11} , In 1999

By design, the M-to-$\bar{M}$ probability upper limit of **10^{-13}** was achieved.

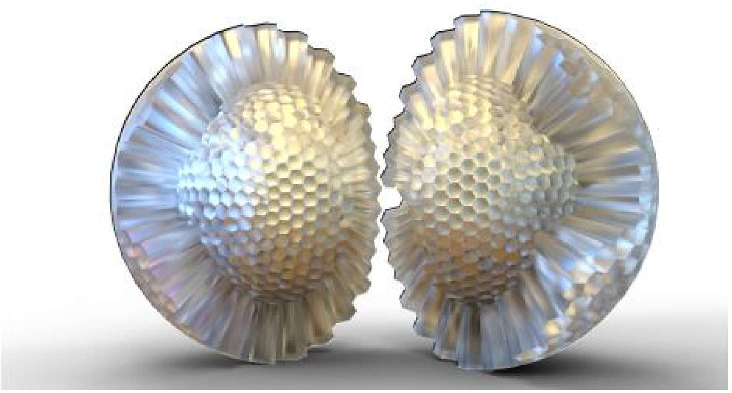

Fig. 4 3D rendered image of the ECAL geometry

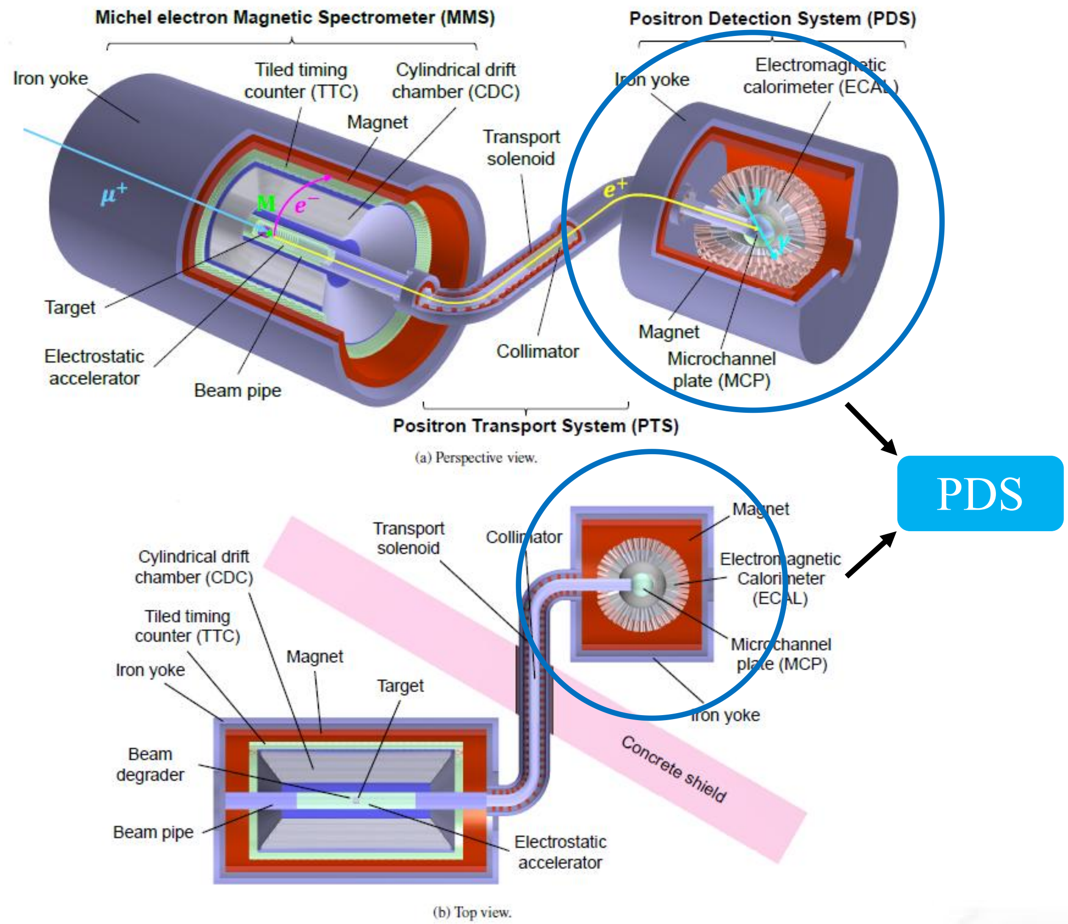

Fig. 5 Overview of MACE detector system. In this presentation, we mainly focus on the positron detection system.

Experiment setup and method

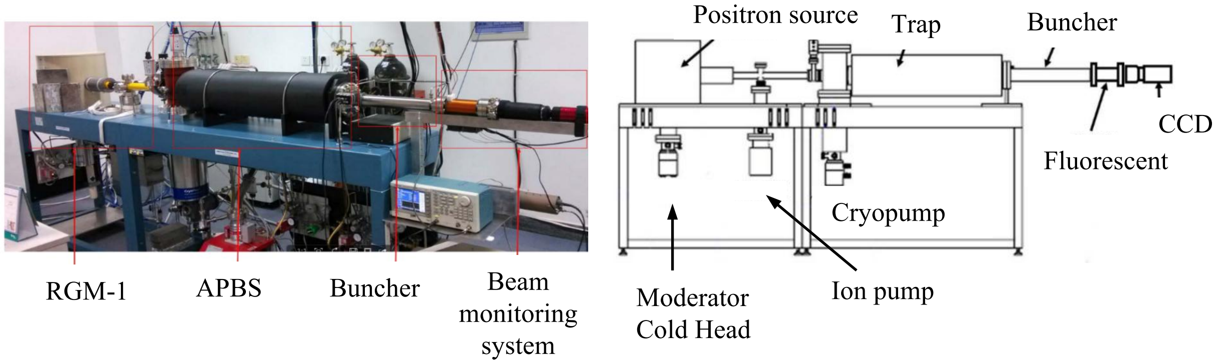

Fig.6 Positron beam based on solid neon moderator.

Beijing intense slow positron beam.

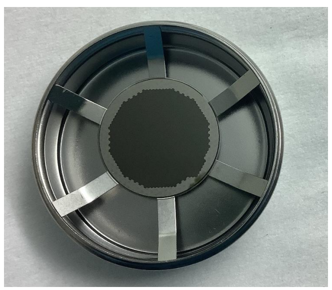

Fig. 7 Φ25 Lead free MCP.

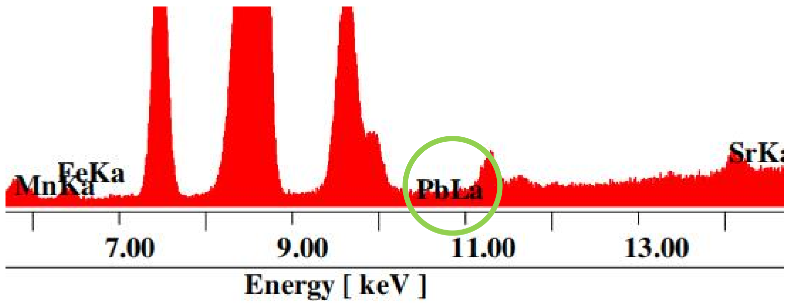

Fig. 8 X-ray fluorescence analysis spectrum of MCP body material

Lead-free MCP enhances detector efficiency.

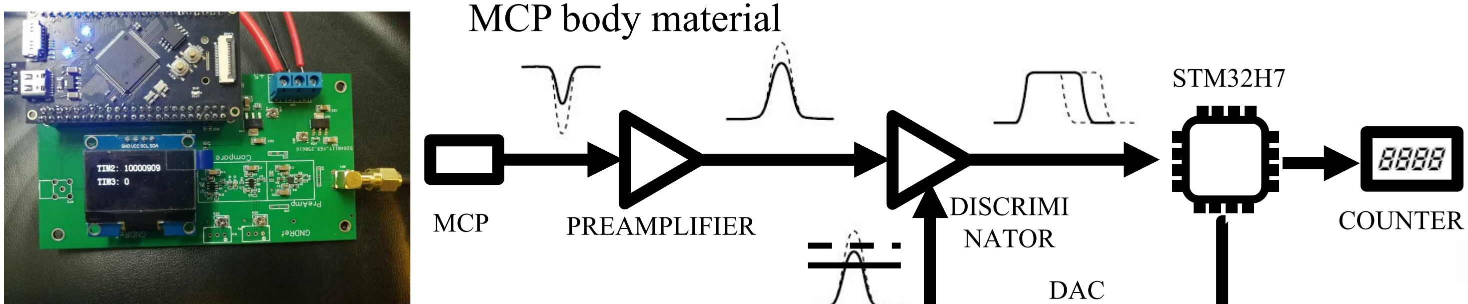

Cost-efficient

Fig. 9 A pulse counting system for the output signal of MCP is implemented using the STM32H7

Performance testing of the PDS

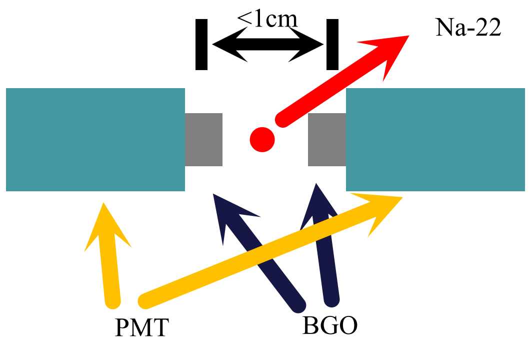

Fig. 10 The time resolution measurement system for BGO scintillation coupled with a PMT.

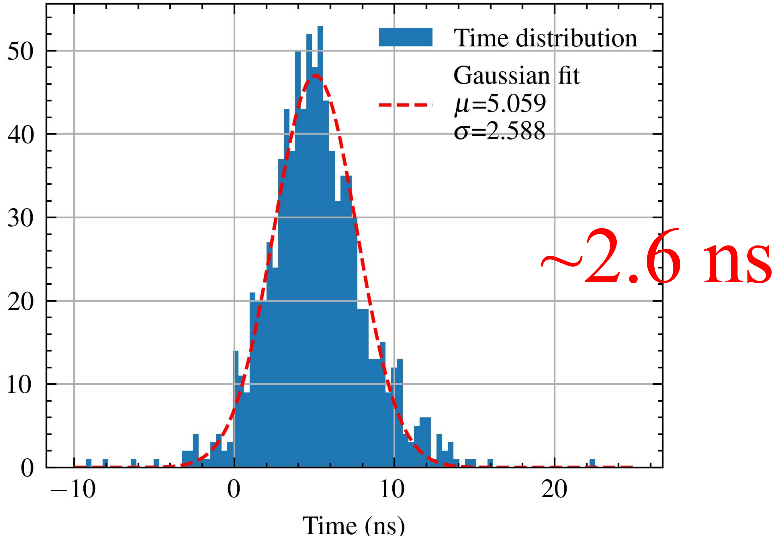

Fig. 11 Time diffirence between the two coincidence PMT.

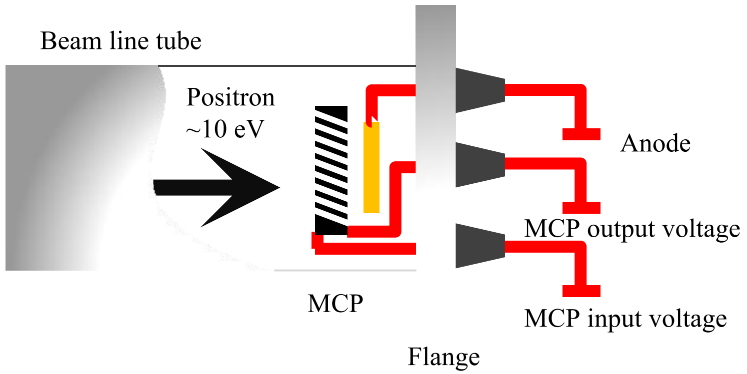

Fig. 12 Schematic of the MCP assembly for positron detection efficiency measurement.

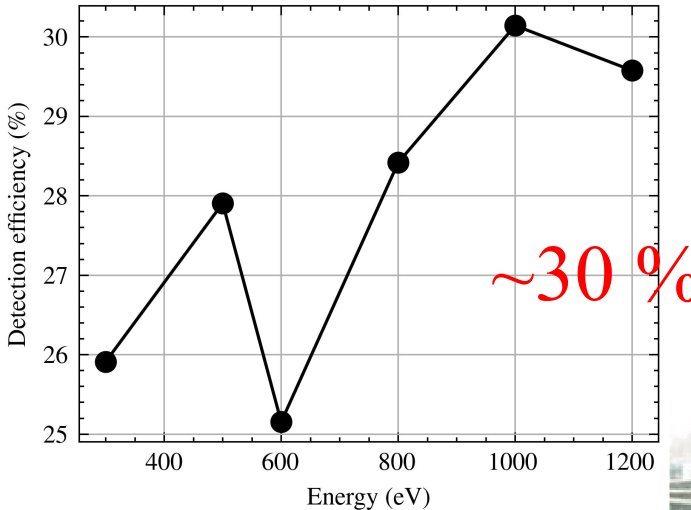

Fig. 13 The positron detection efficiency of MCP under the different impact energy.

Conclusion

- A preliminary test was conducted on the positron detection system. The BGO-PMT achieve a good time resolution for the coincidence of the annihlation gamma-ray process, which is approximately 2.9 ns in our experiment.
- The lead-free MCP achieves a detection efficiency of approximately 30% for positrons with impact energies ranging from 400 eV to 1200 eV. The positron detection efficiency increases with higher impact energies. In the future experiments, a delay line anode or multi-anode will be used to acquire the spacial information of the detected particles.

Thanks